Cell. Mol. Life Sci. 65 (2008) 631 – 643
1420-682X/08/040631-13
DOI 10.1007/s00018-007-7478-z

Cellular and Molecular Life Sciences

Research Article

Accessibility of a critical prion protein region involved in strain recognition and its implications for the early detection of prions

J. Yuan[a], Z. Dong[a], J.-P. Guo[b], J. McGeehan[c], X. Xiao[a], J. Wang[a], I. Cali[a], P. L. McGeer[b], N. R. Cashman[d], R. Bessen[e], W. K. Surewicz [f], G. Kneale[c], R. B. Petersen[a, g], P. Gambetti[a] and W. Q. Zou[a, *]

[a] Department of Pathology and National Prion Disease Pathology Surveillance Center, Case Western Reserve University, 2085 Adelbert Road, Cleveland, Ohio 44106 (USA), Fax: +1-216-368-2546,
e-mail: wenquan.zou@case.edu
[b] Kinsmen Laboratory of Neurological Research, University of British Columbia, Vancouver, BC V6T 1Z3 (Canada)
[c] Biophysics Laboratories, Institute of Biomedical and Biomolecular Sciences, University of Portsmouth, Portsmouth, PO1 2DT (United Kingdom)
[d] Brain Research Centre, University of British Columbia Hospital, 2211 Wesbrook Mall, Vancouver, BC V6T 2B5 (Canada)
[e] Department of Veterinary Molecular Biology, Montana State University, P.O. Box 173610, Bozeman, Montana 59717 (USA)
[f] Department of Physiology and Biophysics, Case Western Reserve University, Cleveland, Ohio 44106 (USA)
[g] Department of Neuroscience, Case Western Reserve University, 2085 Adelbert Road, Cleveland, Ohio 44106 (USA)

Received 17 October 2007; received after revision 5 December 2007; accepted 14 December 2007
Online First 15 January 2008

Abstract. Human prion diseases are characterized by the accumulation in the brain of proteinase K (PK)-resistant prion protein designated PrP27 – 30 detectable by the 3F4 antibody against human PrP109 – 112. We recently identified a new PK-resistant PrP species, designated PrP*[20], in uninfected human and animal brains. It was preferentially detected with the 1E4 antibody against human PrP 97 – 108 but not with the anti-PrP 3F4 antibody, although the 3F4 epitope is adjacent to the 1E4 epitope in the PrP*[20] molecule. The present study reveals that removal of the N-terminal amino acids up to residue 91 significantly increases accessibility of the 1E4 antibody to PrP of brains and cultured cells. In contrast to cells expressing wild-type PrP, cells expressing pathogenic mutant PrP accumulate not only PrP*[20] but also a small amount of 3F4-detected PK-resistant PrP27 – 30. Remarkably, during the course of human prion disease, a transition from an increase in 1E4-detected PrP*[20] to the occurrence of the 3F4-detected PrP27 – 30 was observed. Our study suggests that an increase in the level of PrP*[20] characterizes the early stages of prion diseases.

Keywords. Prion protein, prion disease, epitope, gene 5 protein, neuroblastoma cell, Creutzfeldt-Jakob disease.

* Corresponding author.

Prions, associated with a group of fatal neurodegenerative disorders called prion diseases or transmissible spongiform encephalopathies, are composed largely of an abnormal proteinase K (PK)- resistant prion protein (PrP^{Sc}) [1]. PrP^{Sc} is derived from a PK-sensitive cellular PrP (PrP^{C}) through an alpha helix into beta sheet structural transition. The detailed molecular mechanism resulting in the conversion of PrP^{C} into PrP^{Sc} has not been elucidated [2]. According to the seeding model [3], this conversion is triggered by PrP^{Sc} seeds that are either introduced by exogenous infection in diseases such as kuru, iatrogenic Creutzfeldt-Jakob disease (CJD) and variant CJD, or formed by endogenous PrP^{Sc} molecules in spontaneous prion diseases such as sporadic CJD and various familial prion diseases. Our recent study demonstrated that small amounts of PK-resistant PrP aggregates are present in uninfected human and animal brains [4], providing experimental evidence for the hypothesis that silent prions or prion precursors may be present at a low level in the normal brain [3, 5].

The two PK-resistant PrP fragments identified in normal human brain by Western blot migrate at ~18 and ~20 kDa after deglycosylation and are termed PrP^{*18} and PrP^{*20}, respectively. They differ from the two major PK-resistant PrP27–30 fragments in CJD patients including PrP^{Sc} type 1 and type 2 [4, 6], which migrate at ~ 21 and ~19 kDa and have the N-terminal starting sites at residues 82 and 97, respectively [7]. PrP^{Sc} type 1 and type 2 are readily detected with the anti-PrP 3F4 monoclonal antibody, which recognizes an epitope between amino acids 109 and 112 of the human PrP [6–9]. While PrP^{*18} is detergent insoluble and PK resistant [4], it shares a similar molecular mass with the detergent-soluble and PK-sensitive C1 PrP^{C} polypeptide, which is cleaved by an endoproteinase at residue ~111 or ~112 of the prion protein [10]. Therefore, PrP^{*18} is likely devoid of the 3F4 epitope. However, it was surprising that although containing the 3F4 epitope, PrP^{*20} was barely detected with the anti-PrP 3F4 antibody and was immunoreactive with the anti-PrP 1E4 antibody, which recognizes human PrP sequence between 97 and 108. The structural basis for the inaccessibility of 3F4 to its epitope in the PrP^{*20} fragment is unclear. Moreover, the differences in the PK-resistant PrP species between neuronal cells expressing wild-type and mutant PrP, and the pathophysiological significance of PrP^{*20} in the pathogenesis of prion diseases remain to be determined.

Here we compared the accessibility of 1E4 and 3F4 antibodies to their epitopes in the full-length and N-terminally truncated human PrP from *Escherichia coli*, cultured human neuronal cell lines, and brain tissues obtained at biopsy and autopsy. We observed that the N-terminal sequences affect the accessibility of the two adjacent epitopes differently. The 3F4 epitope is highly accessible in the full-length PrP molecules from the brain and cell lines but is decreased after removing 74 or more N-terminal residues. In contrast, the accessibility of the 1E4 epitope in the full-length PrP of the brain and cultured cells is low, but is increased after removing 74 or more residues from the N terminus. Furthermore, the PrP^{Sc} type 2 that is 15 residues shorter than PrP^{Sc} type 1 at its N terminus has higher immunoreactivity with 1E4 than PrP^{Sc} type 1. Through the use of cell models, we showed that the pathogenic mutant PrP, with threonine (T) changed to alanine (A) at residue 183 (PrP^{T183A}) or phenylalanine (F) to serine (S) at residue 198 (PrP^{F198S}), linked to familial prion diseases [11–13], forms in addition to the 1E4-detected PrP^{*20}, a small amount of the 3F4-detected PrP27–30 upon treatment with PK at a concentration of 50 μg/ml. By screening brain samples obtained at biopsy from CJD-suspected subjects, we identified a group of patients whose biopsy brain tissues showed a significant increase in the level of PrP^{*20}, compared to negative controls, but they were negative for PrP^{Sc} with 3F4. One of these cases turned out to be CJD, evidenced by the occurrence of PrP^{Sc} detected by 3F4 in the autopsy brain tissues $1^{1}/_{2}$ years after the initial biopsy.

Materials and methods

Reagents and antibodies. Phenylmethylsulfonyl fluoride (PMSF), PK, N, N'-diisopropylcarbodiimide, 1-hydroxybenzotriazole, trifluoroacetic acid, piperidine, triisobutylsilane, and dichloromethane were purchased from Sigma (St. Louis, MO). Peptide N-glycosidase F (PNGase F) was purchased from New England Biolabs (Beverly, MA) and used according to the manufacturer's protocol. Reagents including Amino-PEG cellulose membranes and Fmoc-amino acids were obtained from Intavis (San Marcos, CA). N-α-Fmoc-O-benzyl-L-phosphoserine and N-α-Fmoc-O-benzyl-L-phosphothreonine were purchased from AnaSpec (San Jose, CA). Reagents for enhanced chemiluminescence (ECL Plus) were obtained from Amersham Pharmacia Biotech (Piscataway, NJ). Magnetic beads (Dynabeads M-280, tosylactivated) were from Dynal (Oslo, Norway). Anti-PrP antibodies, including mouse monoclonal antibody 3F4 against human PrP residues 109–112 [8] and mouse monoclonal antibody 1E4 against human PrP97–108 (Cell Sciences, Canton, MA) were also used [4].

Preparation of recombinant human PrP. Recombinant human prion protein PrP23–231 and PrP90–231 were prepared as previously described [14]. In brief,

cDNA coding for human PrP23–231 and PrP90–231 was amplified from a plasmid pVZ21 by polymerase chain reaction. The final constructs coded for appropriate PrP fragments fused to the N-terminal linker containing a His6 tail and a thrombin cleavage site. A Gly-Ser-Asp-Pro extension at the N terminus remained after cleavage of the linker. DNA sequences of all constructs were verified by automated DNA sequencing. The purity of the final products was greater than 98% as judged by SDS-PAGE. The identity of each protein was further confirmed by mass spectrometry. Protein concentration was determined spectrometrically using the molar extinction coefficient ε_{280} of 56 795 and 21 495 $M^{-1}\,cm^{-1}$ for PrP23–231 and PrP90–231, respectively [14].

Preparation of gene 5 protein (g5p). The recombinant g5p was isolated from *E. coli,* transformed with an Ff gene 5-containing plasmid and purified using DNA cellulose affinity plus Sephadex G75 sizing columns as described elsewhere [15]. The purity was >99% as determined by quantitation of Coomassie blue-stained bands on SDS-PAGE.

Brain tissues. Consent to use biopsy and autopsy material for research purposes was obtained for all samples. Autopsy was performed within 20 h after death. Biopsy brain tissues were immediately frozen in liquid nitrogen, then transferred to –80 °C for future use. Clinical data and relevant hospital records were examined. The normal human brains were obtained from subjects free of neurological disorders and PrP mutations indicated by neurohistology, immunohistochemistry, Western blotting, and genetic analysis at the National Prion Disease Pathology Surveillance Center (Cleveland, OH). Hamster brain tissues were from animals infected with either mink prion strain 'Hyper' (HY) or 'Drowsy' (DY) [16].

Preparation of brain homogenate. The 10% (w/v) brain homogenates were prepared in 9 volumes of lysis buffer (10 mM Tris, 100 mM NaCl, 0.5% Nonidet P-40, 0.5% deoxycholate, 10 mM EDTA, pH 7.4). As required, brain homogenates were centrifuged at 1000 g for 10 min at 4 °C to collect the supernatant (S1). For PK digestion, samples were incubated with designated amounts of PK at 37 °C for 1 h and the reaction was terminated through the addition of PMSF at a final concentration of 3 mM and boiling in SDS sample buffer (3% SDS, 2 mM EDTA, 4% β-mercaptoethanol, 10% glycerol, 50 mM Tris, pH 6.8) for 10 min.

Epitope mapping by peptide membrane arrays. The general methods for preparing multiple overlapping peptides bound to cellulose membranes have been described in detail previously [17]. After blocking with 5% skim milk in TBS-T at 37 °C for 2 h, the prion peptide membrane was probed with 1E4 at 1:500 in 1% skim milk for 2 h at 37 °C. The membrane was washed with TBS-T, then incubated at 37 °C with 1:4000 HRP-conjugated sheep anti-mouse IgG for 1 h. After a final wash and developing with ECL Western blotting detection reagent (Amersham Pharmacia), the membrane was visualized by Bio-Rad Fluorescent Imager. The control membrane was probed only with HRP-conjugated sheep anti-mouse IgG without 1E4 antibody.

Cloning and production of cell lines. M-17 human neuroblastoma cells were transfected with the episomal vector CEP4β containing a prion coding sequence using the cationic lipid DOTAP (Roche Applied Science) as previously described [18–20]. The inserted PrP coding sequence, under the control of cytomegalovirus promoter, was either normal or mutant (183A or 198S) with valine (V) at residue 129, a natural polymorphic site in the prion protein gene (*PRNP*). The entire PrP coding sequence was amplified from human genomic DNA using the following primers: DG2, 5' GTACTGA**GAATTC**GCAGTCATTATGGCGAACCTTGG3' and DG1, 5'GTACTGA**GGATCC**TCCTCATCCCACTATCAGGAAGA 3'. The underlined sequences correspond to the *PRNP* sequences, nucleotides 41–70 and 792–814, respectively according to the reported sequence [21]. Using the EcoRI and BamHI sites (bold face) in the primers, the coding sequence was cloned into the bacterial plamid pVZ1 [18]. Site-directed mutagenesis was used to create the 183A and 198S mutant sequences (BioRad MutaGene phagemid *in vitro* mutagenesis kit). Transfected cells were grown as bulk selected hygromycin-resistant cultures at 37 °C in OPTI-MEM with 5% calf serum supplement, iron-enriched (GIBCO-BRL) and 500 μg/ml hygromycin B (Calbiochem, La Jolla, CA). For each experiment, cells were removed from the flask with trypsin, and counted; the same number of cells from each cell culture were seeded onto Petri plates. They were incubated overnight to ~95% confluence in complete medium supplemented with serum and antibiotics.

Cell lysis. After removal of the medium, cells were rinsed three times with PBS and lysed in 1.2 ml lysis buffer on ice for 30 min. The cell lysates were centrifuged at 1000 *g* for 10 min at 4 °C to remove nuclei and cellular debris. The supernatant was incubated with 5.5 ml pre-chilled methanol at –80 °C for 2 h and centrifuged at 14 000 *g* for

30 min at 4 °C. The pellet was resuspended in 100 µl lysis buffer.

Specific capture of abnormal PrP by g5p. The g5p molecule (100 µg) was conjugated to 7×10^8 tosyl activated magnetic beads in 1 ml of PBS at 37°C for 20 h [22]. The g5p-conjugated beads were incubated with 0.1 % bovine serum albumin (BSA) in PBS to block non-specific binding. The prepared g5p beads were stable for at least 3 months at 4 °C. The specific capture of PrP^{Sc} by g5p was performed as described elsewhere [22, 23] by incubating S1 fractions and g5p-conjugated beads (10 µg g5p/6×10^7 beads) in 1 ml binding buffer (3 % Tween-20, 3 % NP-40 in PBS, pH 7.5). After incubation with constant rotation overnight at room temperature, the PrP-containing g5p beads were collected with an external magnetic force and all unbound molecules in the solution were removed. Following three rinses in the wash buffer (2 % Tween-20 and 2 % Nonidet P-40 in PBS, pH 7.5), the g5p beads were resuspended in SDS sample buffer (3 % SDS, 2 mM EDTA, 10 % glycerol, 50 mM Tris, pH 6.8) and heated at 95 °C for 5 min to release bound proteins.

Western blot analysis. Samples were resolved on 15 % Tris-HCl Criterion pre-cast gels (Bio-Rad) for SDS polyacrylamide gel electrophoresis at 150 V for ~80 min. The proteins on the gels were transferred to Immobilon-P membrane (PVDF, Millipore) for 2 h at 70 V. The membranes were incubated for 2 h at room temperature with either 3F4 (1:40 000) or 1E4 (1:500) as primary antibody for probing the PrP molecule. Following incubation with HRP-conjugated sheep anti-mouse IgG at 1:3000, the PrP bands were visualized on Kodak film by the ECL Plus in accordance with the manufacturer's protocol.

Results

N-terminal sequences of PrP differentially affect the accessibility of 1E4 and 3F4 antibodies to the two adjacent epitopes. To elucidate the structural properties of the PrP fragment detected by 1E4, the accessibility of the antibody to the full-length and N-terminally truncated recombinant human PrP was first compared by using Western blot analysis. Equal amounts of recombinant PrP including a full-length PrP(23–231) and an N-terminally truncated PrP(90–231) were probed with 1E4 and 3F4. While the band intensity of full-length PrP detected by 3F4 was slightly higher than that recognized by 1E4 (15.41 ± 3.79 vs 11.57 ± 2.69, $p = 0.23 > 0.05$, $n = 3$), there was no significant difference in band intensities for the truncated PrP(90–231) (15.37 ± 3.33 vs 15.41 ± 3.79, $p = 0.71 > 0.05$, $n = 3$) (Fig. 1a). This suggests that the 1E4 and 3F4 epitopes are equally exposed in the N-terminally truncated PrP but the accessibility of the 1E4 epitope is slightly lower than that of the 3F4 epitope in the full-length PrP molecule.

Immunoblots of the uninfected human brain samples demonstrated that two major PrP bands reacted with both the 3F4 and 1E4 antibodies after deglycosylation with PNGase F: an upper band migrating at ~26–28 kDa represents deglycosylated full-length PrP, and a lower band migrating at ~20–22 kDa represents deglycosylated N-terminally truncated PrP [4, 24]. The endogenous N-terminal cleavage sites of the latter have been mapped to the region between residues 80 and 100 [24]. The intensities of the two bands recognized by the two antibodies were compared. 1E4 has a much greater accessibility to the N-terminally truncated PrP than 3F4 (2.37 ± 0.61 vs 0.99 ± 0.36, $p = 0.008 < 0.01$, $n = 4$). By contrast, 3F4 has a slightly greater accessibility to the full-length PrP than 1E4 in the normal human brain samples (2.31 ± 0.91 vs 1.34 ± 0.29, $p = 0.089 > 0.05$, $n = 4$) (Fig. 1b). The mobility of the 1E4-detected truncated form was greater than that detected by 3F4 (20 kDa vs 21–22 kDa) (Fig. 1b). Since it shares similar gel mobility with the PK-resistant PrP^{*20}, the lower PrP band detected with 1E4 possibly contains not only a PrP species sensitive to exogenous PK digestion but also PrP^{*20}.

The differences in the accessibility of the two antibodies to PrP in cell lysates treated with PNGase F were investigated using cultured human neuronal cells expressing wild-type human PrP (PrP^{Wt}). Although the intensity of the N-terminally truncated PrP was higher in the 1E4 blot, the accessibility of the 1E4 epitope in the full-length PrP showed a dramatic decrease compared to the 3F4 blot (5.29 ± 3.83 vs 17.01 ± 7.62, $p = 0.015 < 0.05$, $n = 5$) (Fig. 1c). The full-length PrP became visible only in the over-exposed 1E4 blot (data not shown).

N-terminal sequences between residues 82 and 91 are involved in regulating the accessibility of the 1E4 epitope. To further define the N-terminal sequences that affect the accessibility of 1E4 and 3F4 antibodies, the PK-treated PrP^{Sc} from the two hamster-adapted mink prion strains called 'Hyper' (HY) and 'Drowsy' (DY), as well as human PrP^{Sc} type 1 and type 2 found in sporadic CJD, were probed with the two antibodies. It has been demonstrated that after PK treatment, DY forms a 19 to 20-kDa PK-resistant core fragment with the main N-terminus at residue Gly-92, whereas HY forms ~21-kDa PK-resistant core fragments with a major N terminus at Gln-Gly-Pro located in the

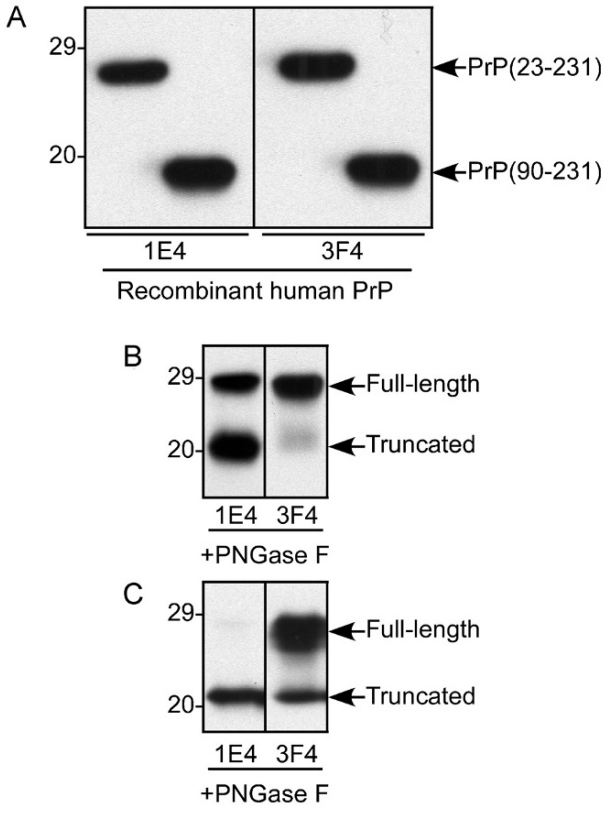

Figure 1. Comparison of accessibility of 1E4 and 3F4 antibodies to the full-length and N-terminally truncated human PrP. (*A*) Recombinant full-length and N-terminally truncated human PrP(23–231) and PrP(90–231). (*B*) Deglycosylation of PrP from normal human brain treated with PNGase F. (*C*) Deglycosylation of PrP from cultured human neuroblastoma cells expressing PrP^{Wt} treated with PNGase F.

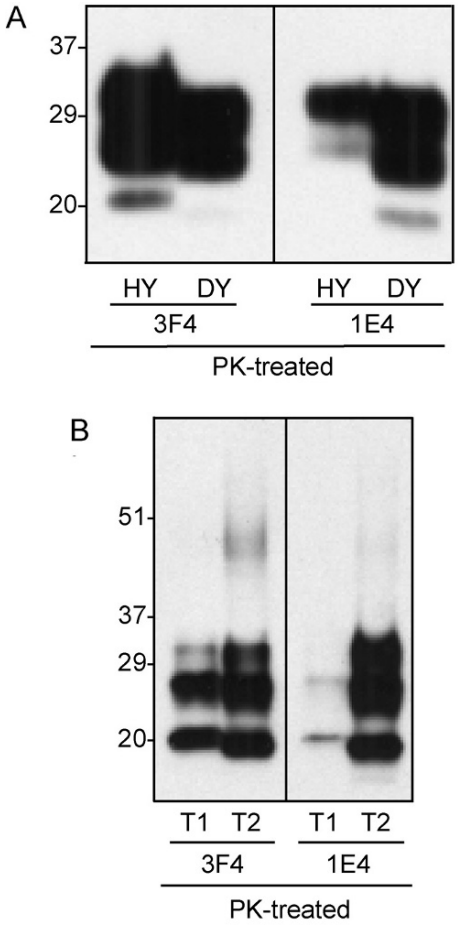

Figure 2. Comparison of accessibility of 3F4 and 1E4 to PK-treated PrP^{Sc}. (*A*) PK-treated PrP^{Sc} from hamster-adopted mink prion strains 'Hyper' (HY) and 'Drowsy' (DY). (*B*) PK-treated PrP^{Sc} from sCJD type 1 (T1) and type 2 (T2).

octapeptide repeat region extending from Pro-52 to Gln-91 [16]. The accessibility of 1E4 to the PK-treated DY PrP fragment was slightly greater than that of 3F4 (4.03 ± 1.55 vs 3.42 ± 1.06, $p = 0.408 > 0.05$, $n = 7$), and the 1E4 reacted not only mainly with the diglycosylated and monoglycosylated PrP (upper and middle bands) but also with an unglycosylated PrP (lower band) (Fig. 2a). However, in the PK-treated HY strain, the accessibility of 1E4 to PrP was much lower than that of 3F4 (2.03 ± 0.91 vs 4.31 ± 1.16, $p = 0.0015 < 0.01$, $n = 7$). Compared to 3F4, 1E4 detected approximately 56 % of the upper band and ~ 37 % of the middle band. The lower band of PK-treated HY was virtually undetectable with 1E4 (Fig. 2a). These results clearly indicate that removal of N-terminal amino acids up to residue 91 dramatically increases the accessibility of the 1E4 epitope. Since the decrease in the PrP intensity was more obvious in the monoglycosylated middle band than in the diglycosylated upper band of HY PrP, it is conceivable that the accessibility of the 1E4 epitope between the two fragments differs. This could be due to a different structure in this area or to a different glycosylation effect. In addition, since the mobility of the PK-resistant DY PrP fragment is similar to that of PrP^{*20} (19–20 kDa vs 20 kDa), the possibility cannot be ruled out that the small difference in the band intensity detected with 1E4 and 3F4 (4.03 ± 1.55 vs 3.42 ± 1.06) is derived from the presence of a small amount of PrP^{*20}.

Compared to 3F4, 1E4 showed a much lower accessibility to PrP^{Sc} type 1 (0.93 ± 0.32 vs 2.23 ± 0.67, $p = 0.0043 < 0.01$, $n = 5$) but a slightly greater accessibility to PrP^{Sc} type 2 (3.62 ± 0.86 vs 2.66 ± 1.01, $p = 0.143 > 0.05$, $n = 5$) (Fig. 2b), which is consistent with the results observed in hamster HY and DY strains. Therefore, at least in human PrP^{Sc}, the N-terminal sequence between residues 82 and 97 significantly interferes with the binding of 1E4 to PrP97–108. In addition, the sequence between residues 97 and 108 also partially affects the accessibility of 3F4 to its epitope, inasmuch as the accessibility of 1E4 to PrP^{Sc} type 2 was greater than that of 3F4.

Amino acids 93 to 96 have no significant effect on the accessibility of 1E4 to its epitope in the human PrP. The 1E4 antibody product description indicates that the 1E4 antibody was generated by immunization of a Prnp 0/0 mouse with a peptide GQWNKPSKPKTN, corresponding to the bovine PrP sequence 108–119. The sequence of this peptide corresponds to the human PrP 97–108. As shown above, the 1E4 epitope in PrP^{Sc} is exposed in the hamster PrP27–30 with an N-terminal start site at Gly-92 and in the human PrP27–30 with an amino start site at Ser-97. However, whether or not the amino acids between residues 93 and 96 in the human PrP influence the accessibility of the 1E4 epitope has not been ascertained. The precise location of the 1E4 epitope in the human PrP molecule has also not been determined. To identify the origin of this unique immunoreactivity, investigation of the precise location of the 1E4 epitope in human PrP would be required. Human prion peptides from residues 92 to 105 were synthesized from 13 to 4 amino acids in length onto cellulose membranes, gradually removing amino acids one by one either from the N- or the C-terminus. As shown in Figure 3, the immunoreactivities of 1E4 with the various prion peptides were separable into five groups based on their staining intensity. The level 1 group included six peptides with the highest immunoreactivity, and the shortest peptide containing residues 98–105 (Fig. 3; level 1 panel, spot 3C). Removing the N-terminal amino acids one by one from residues 93 to 97 resulted in no significant decrease in the PrP staining intensity (Fig. 3). A slight decrease was noted for 1E-reacting prion peptide spot from residues 94 to 105 (Fig. 3). However, the immunoreactivity obviously decreased from the level 2 group to level 4 following sequential removal of the C-terminal amino acids from residue 105 to residue 100 (Fig. 3). The level 5 group included the peptides without observable immunoreactivity. Peptides yielding the highest reactivity with 1E4 generally contained the sequences PrP(98–105), QWNKPSKP, and the lowest reactivity was from the PrP(97–101) peptide, containing the four amino acids SQWN. These results confirm that the 1E4 epitope is adjacent to the N terminus of the 3F4 epitope in human PrP. Moreover, the N-terminal sequence between residues 93 and 96 of the 1E4 epitope does not affect 1E4 accessibility. In contrast, either addition, deletion or both of one or more C-terminal amino acids dramatically decreases immunoreactivity.

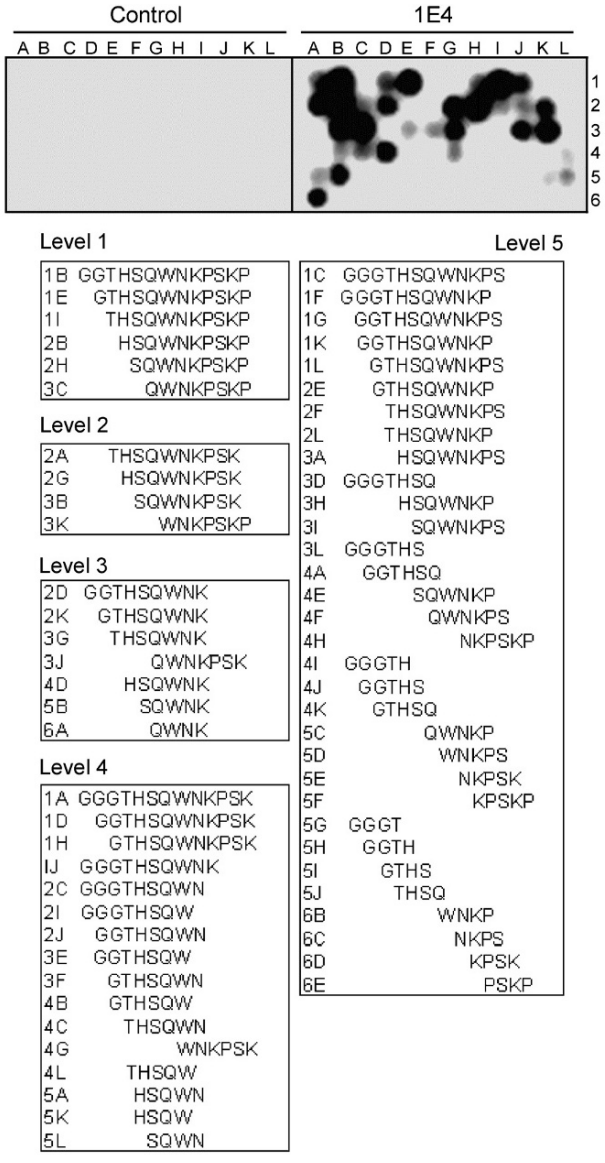

Figure 3. Epitope mapping by peptide membrane arrays. Based on the primary epitope probing of the 1E4 antibody on 13-mer peptide array membranes of full PrP sequence (data not shown), the fragment from the 92nd to 105th residues of PrP was chosen for further epitope probing. The peptides with lengths from 13-mer to 4-mer in this region were synthesized on amino-PEG cellulose membranes with one amino acid shift each from the N or C terminus. Five populations of prion peptides were grouped based on the intensity of spots. The Level 1 group included peptides that had highest intensity, while the level 5 group included the peptides without immunoreactivity.

Human neuronal cells expressing pathogenic mutant PrP accumulate the 1E4-detected PrP*20 and a small amount of the 3F4-detected PrP27–30. Neuroblastoma cells expressing various human PrP mutants have been widely used to study the properties of mutant PrP linked to naturally occurring familial prion diseases [18–20]. Here, we asked whether the mutant PrP can also form PrP*20 in cultured neuronal cells and whether any differences exist in the accumulation of PK-resistant PrP species between cells expressing PrP^{Wt} and pathogenic PrP mutants. Human neuroblastoma cells (M17) expressing either PrP^{Wt}, PrP^{T183A}, or PrP^{F198S} were used in our study because

the two mutations are linked to familial CJD and Gerstmann-Sträussler-Scheinker syndrome (GSS), respectively [11–13, 25].

Probed with the 3F4 antibody, PrP^{Wt} migrated as three major bands of 36–48 kDa diglycosylated, 30–35 kDa monoglycosylated, and 27–28 kDa unglycosylated forms (Fig. 4a). In contrast, a major single band migrating at 28–33 kDa, corresponding to the monoglycosylated PrP, was detectable in the cell lysates containing PrP^{T183A} (Fig. 4a). Bands migrating at 37–45 kDa and 33–36 kDa corresponding to the diglycosylated and monoglycosylated forms, respectively, were detected in the cell lysates containing PrP^{F198S}; the unglycosylated form was virtually undetectable (Fig. 4a). The PrP profiles observed using the 3F4 antibody are consistent with the previous observations [19, 20]. However, the PrP bands were very faint when the three different cell lysates were probed with 1E4 (Fig. 4a), consistent with the notion that the 1E4 epitope is mostly blocked in the full-length PrP of the cultured cells (see above).

With conventional Western blot analysis, PrP was undetected with either the 3F4 or 1E4 antibodies in the wild-type or mutated PrP-containing cell lysates after PK treatment at 50 μg/ml, 37 °C for 1 h, a condition used for detecting human PrP^{Sc} [26]. Several faint PK-resistant PrP bands could be detected only with 1E4 after treatment with low concentrations of PK such as 5 or 10 μg/ml (data not shown). To search for small amounts of abnormal PrP species that are resistant to PK at 50 μg/ml, the cell lysates containing either wild-type or mutant PrP were incubated with g5p, a single-stranded DNA binding protein that is able to capture abnormal PrP from prion-infected and uninfected brains [4, 23]. After incubation, the samples were treated with 50 μg/ml PK at 37 °C for 1 h, and further treated with PNGase F as required, prior to SDS-PAGE and immunoblotting with either 1E4 or 3F4.

In the samples from wild-type cells, four PrP bands were observed on the blot probed with 1E4 after PK treatment, migrating at ~31–37 kDa, ~23–27 kDa, ~19–20 kDa, and ~7–8 kDa (Fig. 4b, upper panel). The first three bands correspond to diglycosylated, monoglycosylated, and unglycosylated PrP, respectively, which are similar to PrP27–30. The band migrating at ~7–8 corresponds to the PrP7–8 fragment, which is generally characteristic of GSS. In contrast, in the cell lysates containing PrP^{T183A}, 1E4 revealed an intense band migrating at 23–26 kDa and a faint band at 7–8 kDa (Fig. 4b, upper panel). The profile of PrP^{F198S} was different from that of either PrP^{Wt} or PrP^{T183A}. PrP^{F198S} had three PK-resistant bands: a ~32 to 39 kDa band corresponding to diglycosylated PrP, an ~26 to 29 kDa band corresponding to monoglycosylated PrP, and an ~7 to 8 kDa band observed when probed with 1E4 (Fig. 4b, upper panel). The migration of both diglycosylated and monoglycosylated PrP^{F198S} was slower than that for PrP^{Wt} (Fig. 4b, upper panel), suggesting that the mutation affects glycosylation or N-terminal cleavage of the protein, or both. In addition, the mobility of the monoglycosylated PrP^{F198S} was slower than that of monoglycosylated PrP^{T183A}. The unglycosylated PrP migrating at ~19–20 kDa was not detectable in either PrP^{T183A} or PrP^{F198S}. After deglycosylation with PNGase F, a major PrP band migrating at ~19–20 kDa was detected in all samples. The latter band corresponds to PrP^{*20} identified in normal brains [4]. About one-third of the monoglycosylated PrP from PrP^{T183A} was not completely deglycosylated, remaining at ~23–26 kDa. Perhaps this resistance to deglycosylation arises from an abnormal glycosylation induced by this pathogenic mutation. PrP7–8 was present in all three cell types expressing wild-type and mutated PrP, and no significant changes in the mobility and intensity were observed compared to the samples without PNGase F treatment (Fig. 4b, upper panel). The mobility of PrP^{*20} from PrP^{T183A} was slightly faster than that of PrP^{*20} from PrP^{Wt} and PrP^{F198S} (Fig. 4b), suggesting that the PrP^{*20} fragment may vary from wild-type and mutated PrP or between different PrP mutants.

In contrast to the blots probed with 1E4, PrP was undetectable in the samples containing PrP^{Wt} and PrP^{F198S} on the 3F4-probed immunoblot, but two faint bands were present migrating at ~30–32 kDa and ~23–26 kDa in the PrP^{T183A} lysates (Fig. 4b, lower panel). Based on the protein molecular mass, the former corresponds to the undigested full-length monoglycosylated PrP that was undetected with 1E4 (Fig. 4b). The latter band represents a partially PK-resistant form of the monoglycosylated PrP. The band migrating at ~23–26 kDa detected with 3F4 corresponds to that detected by 1E4 with respect to its mobility. Interestingly, after PNGase F treatment, a faint band migrating at ~19–20 kDa was detected by 3F4 in the PrP^{T183A} or PrP^{F198S} cell lysates, but not in PrP^{Wt} cell lysates (Fig. 4b, lower panel). In addition, the migration of the 3F4-detected PrP27–30 from PrP^{T183A} was also slightly farther than that from PrP^{F198S}; being similar to the behavior of that detected by 1E4. Since it is detected by 3F4, this band should correspond to the PK-resistant deglycosylated PrP27–30 observed in prion-infected brains and cells. Compared to the blot probed with 1E4, the intensity of PrP detected with 3F4 was much less. However, the 1E4-detected PrP^{*20} in PrP^{T183A} and PrP^{F198S} cell lysates exhibited gel mobility similar to that of a band detected by 3F4 at ~19–20 kDa. Therefore, cells

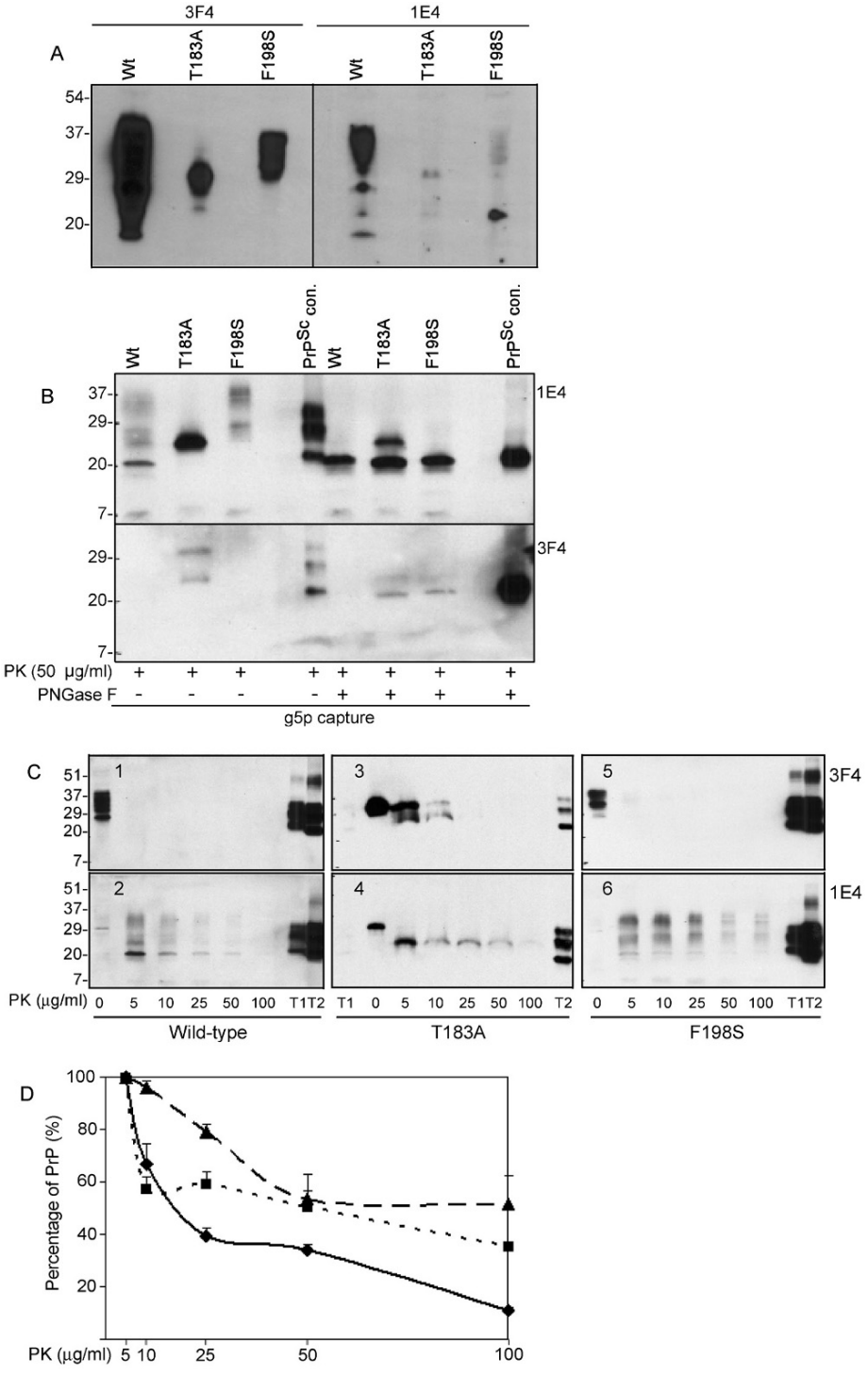

Figure 4. Western blot analysis of PrP^{Wt}, PrP^{T183A}, and PrP^{F198S} with 3F4 and 1E4. (*A*) PrP from cell lysates containing PrP^{Wt}, PrP^{T183A}, or PrP^{F198F}. The blot was probed with either 3F4 or 1E4. (*B*) PrP captured by g5p from cell lysates containing PrP^{Wt}, PrP^{T183A}, and PrP^{F198S}, probed with 1E4 or 3F4. (*C*) PK resistance of PrP captured by g5p from cell lysates containing PrP^{Wt}, PrP^{T183A}, and PrP^{F198S}. T1, PrP^{Sc} type 1 control. T2: PrP^{Sc} type 2 control. (*D*) Percentage of PrP treated with different PKs at 5 µg/ml PK as a function of various PK concentrations. The solid line with diamonds represents PrP^{Wt}, the dashed line with triangles represents PrP^{T183A}, and the dotted line with squares represents PrP^{F198S}.

expressing pathogenic mutant PrP generate the 1E4-detected PrP^{*20} and an extremely low amount of the 3F4-detected PrP27–30 following PK treatment.

The PK resistance of PrP^{*20} from PrP^{Wt}, PrP^{T183A}, and PrP^{F198S} was compared. The g5p-captured PrP from the cell lysates of the three different cell lines was treated with varying concentrations of PK ranging from 5 to 100 µg/ml at 37 °C for 1 h. The 3F4 antibody again showed distinct PrP profiles in the three untreated cell lysates (Fig. 4c, panels 1, 3 and 5), as seen above. However, no convincing PrP bands were detectable with 3F4 in the PrP^{Wt} or PrP^{F198S} lysates treated with PK at 5 µg/ml or higher (Fig. 4c, panels 1 and 5). Two PrP bands were detected only in the PrP^{T183A} cell lysates treated with low amounts of PK at 5 and 10 µg/ml. An upper band was found migrating at

~30–32 kDa corresponding to undigested full-length monoglycosylated PrP and a lower band migrating at ~23–26 kDa corresponding to a partially PK-resistant PrP (Fig. 4c, panel 3). Although the sample loads were identical, the PrP intensity revealed with 1E4 was less than that detected by 3F4 in the untreated samples (Fig. 4c, panels 2, 4, and 6). The 1E4 antibody recognized several PrP bands in the three PK-treated cell lysates (Fig. 4c, panels 2, 4, and 6). The profiles of the PK-resistant PrP bands detected by 1E4 were similar to those shown in Figure 4b. Interestingly, the 1E4-detected PrP^{*20} from PrP^{T183A} and PrP^{F198S} lysates was seen in the samples treated with 100 μg/ml PK (Fig. 4c, panels 4 and 6). In contrast, PrP^{*20} from PrP^{Wt} was virtually undetectable at 100 μg/ml PK treatment (Fig. 4c, panel 2). The ratio of band intensity of PrP treated at 100 μg/ml PK to PrP treated at 5 μg/ml PK was much lower in PrP^{Wt} than in PrP^{T183A} or PrP^{F198S} ($11.18 \pm 1.11\%$ vs $35.85 \pm 0.84\%$, $p = 0.00003 < 0.001$, $n = 3$; $11.18 \pm 1.11\%$ vs $51.88 \pm 10.77\%$, $p = 0.0029 < 0.01$, $n = 3$) (Fig. 4d). This suggests that mutant PrP^{*20} may have greater resistance to PK than does wild-type $PrP^{*20.}$

An increase in the level of the 1E4-detected PrP^{*20} precedes the occurrence of the 3F4-detected PrP27–30. To test the possibility that an increase in the level of PrP^{*20} may represent an early event in the pathogenesis of prion disease, we screened 30 brain biopsy tissues from CJD-suspected patients who tested negative for PrP^{Sc} by 3F4. In the biopsy brain tissues, three CJD-suspected cases revealed a pronounced increase in the level of PrP^{*20}, compared to non-CJD biopsy controls (Fig. 5a). Densitometry analysis of the PrP bands indicated that the increase in PrP^{*20} is statistically significant (CJD-suspected cases ($n = 3$) vs non-CJD cases ($n = 3$): 3.01 ± 0.66 vs 1.51 ± 0.36; $p = 0.0028 < 0.01$). All these cases were clinically observed to have prion-related symptoms, but no detectable prion-related neuropathological changes under light microscopy. Moreover, the use of both Western blotting as well as immunohistochemistry showed that PrP27–30 was not detected with 3F4 antibody.

Remarkably, one of these cases was observed to undergo a transition during a CJD course in which an increase in the level of 1E4-detected PrP^{*20} was the only finding in the frozen brain tissue obtained at biopsy; and the appearance of 3F4-detected PrP27–30 was observed only in the autopsy samples, obtained 1.5 years after the biopsy. No PK-resistant PrP was found using the 3F4 antibody in the frozen frontal cortex and cerebellar tissues obtained at biopsy from the CJD subject, although PrP27–30 was detected in CJD controls (Fig. 5b). In contrast, probing with 1E4, three bands migrating at 21–30 kDa in the frontal cortex sample and at 20–30 kDa in the cerebellar sample became detectable (Fig. 5c), although two faint PrP bands migrating at ~29–30 and ~19–20 were also seen in the non-CJD control in the over-exposed blot (data not shown). Thus, the level of 1E4-detected PrP^{*20} in this case was significantly increased in the biopsy samples, compared to the non-CJD control. To confirm that these protein bands were indeed PrP, the PK-treated frontal cortex sample was further treated with PNGase F to remove the glycans from the protein. After PNGase F treatment, the three bands merged into one band migrating at ~19–20 kDa (Fig. 5d), indicating that the protein detected by 1E4 corresponds to PrP^{*20}. No neuropathological changes were detectable in the biopsy samples.

When the autopsy brain tissues of this case became available, PK-resistant PrP in different brain areas was examined. In the autopsy samples, in addition to the frontal cortex, the 3F4-detected PrP27–30 was also detected in several areas such as the temporal cortex, parietal cortex, insula, thalamus and putamen (Fig. 5e). However, PK-resistant PrP was virtually undetectable in the occipital, cerebellum and brain stem with 3F4. In contrast, greater amounts of PrP were detected with 1E4 in most of the brain areas examined (Fig. 5f). The amount of the 1E4-detected PK-resistant PrP^{*20} in the frontal cortex obtained at autopsy was much greater than that detected in the biopsy sample (Fig. 5c, f).

Discussion

In this study, three observations were made by epitope mapping, characterization of PK-resistant PrP species in uninfected cultured neuronal cells, and examination of PK-resistant PrP in the course of CJD. First, the accessibility of the adjacent epitopes of the 1E4 and 3F4 antibodies between PrP residues 97 and 112 is differently regulated by their neighboring N-terminal sequence. Second, in uninfected cultured cells, both the PrP^{Wt} and PrP mutants form PrP^{*20}. In addition, mutant PrP forms not only PrP^{*20} but also 3F4-detected PrP27–30 after PK treatment. Third, by monitoring the CJD disease course, a significant increase in the level of PrP^{*20} was observed in CJD-suspected cases compared with non-CJD controls, one undergoing a transition from an increase in PrP^{*20} in the biopsy samples to the appearance of PrP27–30 in the autopsy samples.

The PK-resistant PrP^{*20} identified in the normal brain [4], cultured neuronal cells, and brain tissues of early stage CJD (current study) is preferentially detected by 1E4, but not by 3F4. The epitopes of the two anti-

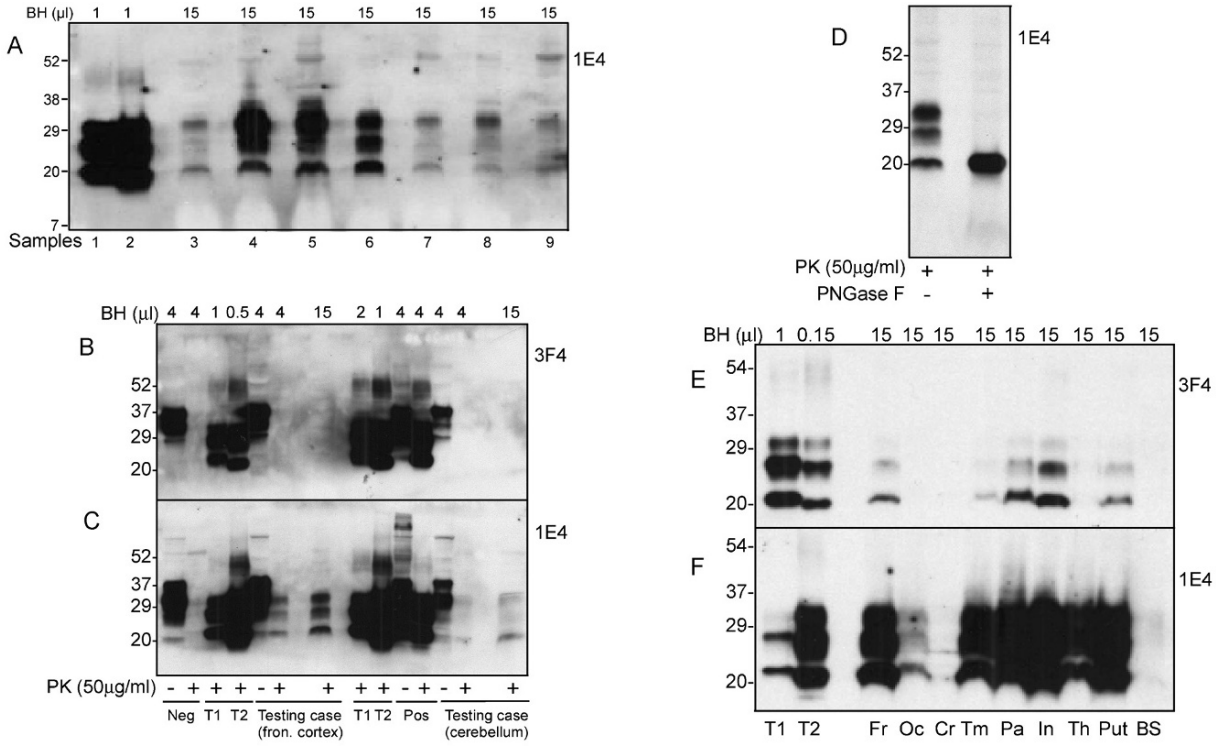

Figure 5. Western blot analysis of PK-resistant PrP in the brain tissues obtained at biopsy and autopsy. (*A*) Western blot analysis of PK-resistant PrP from CJD-suspected and non-CJD cases. Samples 1 and 2, PrP^{Sc} type 1 and 2 controls from frontal cortex. Samples 3–6 were from frontal cortex tissues of CJD-suspected cases except for sample 4 from pulvinar. Samples 3 (frontal cortex) and 4 (pulvinar) were from the same case. Samples 7 and 8 were from frontal cortex with Alzheimer disease used as non-CJD controls. Sample 9 was from normal frontal cortex. BH, brain homogenate. All samples were treated with PK at 50 µg/ml, 37°C for 1 h. (*B, C*) Western blot analysis of samples from a CJD subject obtained at biopsy. PrP from the biopsy samples of the frontal cortex and cerebellum, probed with 3F4 (*B*) or 1E4 (*C*). Neg, non-CJD negative control; T1, PrP^{Sc} type 1 control; T2, PrP^{Sc} type 2 control; Fron., frontal; Pos, CJD-positive control. (*D*) Deglycosylation of the PK-treated biopsy frontal cortex brain homogenate with PNGase F, probed with 1E4. (*E, F*) PK-treated PrP from different brain areas obtained at autopsy probed with 3F4 (*E*) and 1E4 (*F*). Fr, frontal cortex; Oc, occipital cortex; Cr, cerebellum; Tm, temporal cortex; Pa, parietal cortex; In, insula; Th, thalamus; Put, putamen; BS, brain stem.

bodies reside next to each other. This was confirmed by our current peptide membrane arrays. Surprisingly, the accessibility of the two epitopes in the PrP^{*20} molecule is modulated differently by the adjacent flexible N-terminal sequence even on the immunoblot. Several lines of evidence have indicated that the denatured PrP may acquire some structures during Western blotting [20, 27]. We have previously demonstrated that the 6H4 epitope located between residues 144 and 152 of PrP was concealed on the immunoblot after reduction and alkylation of the denatured brain homogenates [27]. It was assumed that certain intramolecular or intermolecular interactions, or both, between the 6H4 epitope and C-terminal reduced and alkylated Cys residues may occur on the PVDF membrane during the Western blot processes. Another anti-PrP antibody 8H4 against human PrP175–185 recognized PrP^{Wt} but not PrP^{F198S} on the immunoblot; yet it binds equally well to native forms of the two proteins [20].

Nuclear magnetic resonance study of recombinant human PrP has revealed that no structure can be assigned to the N terminus of the protein from residues 23 to 124 [28]. However, N-terminal regions encompassing residues 82–124 or 97–124 in PrP^{Sc} type 1 and 2, respectively, become resistant to PK digestion, which suggests that these regions may acquire abnormal structures during conversion of PrP^{C} into PrP^{Sc}. Indeed, the idea has been advanced that the flexible region at the N terminus of PrP90–231 is critical to the conversion of PrP^{C} into PrP^{Sc} [29, 30]. Epitope mapping using ELISA or immunoprecipitation showed that the epitopes from residues 95 to 104 recognized by the Fabs R10, D4 and D13 antibodies, and from residues 109–112 recognized by the 3F4 antibody, were exposed in both PrP^{C} and GdnSCN-denatured PrP27–30 but were cryptic in the undenatured PrP27–30 [9]. In addition, antibodies D13 and 3F4 rapidly lost their immunoreactivity to the recombinant hamster PrP29–231 immobilized on the surface of a sensor chip because of the spontaneous rearrangement of the protein to a conformation characteristic of PrP^{Sc} [31]. Interestingly, these authors inferred from these observations that PrP90–

115 may act as a 'nucleation' point from which conformational change can disseminate to other parts of the protein [31].

We have found that the distinct accessibilities of the 1E4 and 3F4 epitopes in either full-length or N-terminally truncated PrP indicate that although the two epitopes are localized adjacently within the 'nucleation' domain, they are nevertheless not accessible synchronously. Based on the fact that a small amount of 1E4-detected PK-resistant PrP^{*20} is present in uninfected brains and cells, and the additional fact that an increase in its level was observed in the early stage of prion disease, we postulate that the PrP sequence between residues 97 and 108 comprising the 1E4 epitope may act as a 'trigger' for initiating the 'nucleation' of the molecule. Under abnormal conditions such as mutation, the 'triggering domain' from residues 97–108 initiates a structural change of the entire 'nucleation' domain from residues 97–115. This spreads to other parts of the molecule, ultimately generating PrP^{Sc} yielding the 3F4-detected PrP27–30 after PK treatment. Thus, it is possible that the 1E4-detected PrP^{*20} is an immediate precursor of 3F4-detected PrP27–30. In addition to its potential role in triggering nucleation of the protein, the peculiar PrP sequence between residues 90–115 encompassing the two epitopes may also dictate the formation of the different hamster HY and DY as well as human PrP^{Sc} type 1 and 2 prion strains. Interestingly, Tessier and Lindquist [32] have recently identified small elements of primary sequence that govern the nucleation, strain specificity and species barriers of yeast prion Sup35. Given that the PrP sequence between residues ~ 82 and 115 is the PK cleavage site of either PrP^{Sc} type 1 or type 2, it will be important to determine if this region plays a role similar to the prion recognition elements identified in Sup35.

The pathogenic mutations T183A and F198S occur in the two PrP consensus sites for the Asn-linked glycosylation (residues 181–183 and 197–199). T183A mutation of PrP blocks the addition of the first glycan to the Asp residue 181 [11]. PK-resistant heterozygous PrP^{T183A} from a CJD subject exhibited a dominant monoglycosylated and faint diglycosylated and unglycosylated PrP [33]. The small amount of diglycosylated PK-resistant PrP in this case was believed to derive from the normal wild-type PrP allele. Indeed, diglycosylated PrP was undetected, and only a monoglycosylated PrP and a small quantity of the unglycosylated PrP were present in the human neuroblastoma cells expressing homozygous PrP^{T183A} [19]. Although almost all mutant PrP^{T183A} was insoluble in non-ionic detergent buffer, it was uncertain if there were any PK-resistant PrP species in these cells [19]. PK-resistant PrP^{F198S} present in the brain tissues of patients with GSS linked to PrP^{F198S} was found to consist of three major PrP fragments migrating at ~27–29, 18–19, and 8 kDa [34]. The human neuroblastoma cells expressing human PrP^{F198S} showed a greatly increased efficiency of glycosylation at Asp-197 and a slightly increased glycosylation at Asp-181, resulting in a decrease of the unglycosylated isoform; and most of this mutant PrP was recovered in the detergent-insoluble fraction [20]. Three times more PK-resistant PrP^{F198S} than PrP^{Wt} was detected with 3F4 antibody in the insoluble fraction treated with a low concentration of PK of 3.3 μg/ml for 5 min at 37 °C [20].

Using the 1E4 antibody we demonstrated that the uninfected human neuroblastoma cells expressing either PrP^{Wt} or mutant PrP also contain PrP^{*20}. In the full-length PrP^{*20} molecule, the 3F4 epitope is exposed but the 1E4 epitope is concealed. Removal of an N-terminal sequence by PK treatment exposes the 1E4 epitope and blocks the 3F4 epitope. This is consistent with the observation that PK treatment of PrP^{Sc} producing PrP27–30 increases its tendency to form amyloid rods because of a dramatic quaternary structural rearrangement [1]. Therefore, like PrP^{Sc}, the PrP^{*20} molecule possesses a pronounced tendency to form aggregates upon PK treatment, evidenced by the inaccessibility of the 3F4 epitope. On the other hand, this study also raises the important question of whether or not there exists a PrP27–30 molecule which has a concealed 3F4 epitope. In our routine practice at the National Prion Disease Pathology Surveillance Center of Cleveland, Ohio, we observed that there is a subset of PrP^{Sc} that decreases its intensity with 3F4 after PK treatment [X. Xiao and W. Q. Zou, unpublished data]. This may imply that a subset of PrP^{Sc} molecules generates a concealed 3F4 epitope as a result of the removal of the N-terminal region, provided the possibility can be ruled out that these samples have less PK-resistant PrP.

Abnormal PrP species enriched by g5p from the cells expressing pathogenic mutant PrP, in addition to the 1E4-detected PrP^{*20}, also form the 3F4-detected PrP27–30 after the PK treatment. Since PrP^{T183A} and PrP^{F198S} are more resistant than PrP^{Wt} to PK digestion, and only mutant but not wild-type PrP forms the 3F4-detected PrP27–30, it is possible that the most PK-resistant portion of PrP^{*20} is first converted into the PrP27–30. The gel mobility of the 3F4-detected PrP27–30 from PrP^{T183A} is greater than that of PrP^{F198S}, being similar to the gel behavior of PrP^{*20} of PrP^{T183A} and PrP^{F198S}. This might provide experimental evidence that the entire 'nucleation' domain is activated by its N-terminal 'triggering' residues in the pathogenic PrP mutants. Moreover, the demonstration that both wild-type and mutant PrP

contain the 1E4-detected PrP*20 but that only mutant PrP species form the 3F4-detected PrP27–30 in these uninfected human neuronal cells again suggests that the two different PK-resistant species represent the products of two sequential pathogenic processes, and that a mutation occurring in the protein facilitates these processes. Therefore, the formation of PrP*20 may constitute an early event in the formation of PrPSc in the spontaneous prion diseases. It would be interesting to ascertain the two types of PK-resistant PrP species in asymptomatic PrP mutant carriers. To the best of our knowledge, ours is the first study to show that mutant PrP in the uninfected cell models can spontaneously form an abnormal PrP species which generates the 3F4-detectable PrP27–30 after treatment with such a high PK concentration. Whether PrP*20 and PrP27–30 which we identified in these cells are infectious remains to be determined.

Although it is apparent that insoluble aggregates and PK-resistant conformers of PrP are present in uninfected brains [4] and cultured cells (current study), the pathophysiological significance of these prion-like forms remains to be elucidated. A transition from an increase in the level of 1E4-detected PrP*20 to the appearance of the 3F4-detected PrP27–30 in a CJD case further indicates that the accumulation of PrP*20 precedes the deposition of PrPSc. It is possible that the increased PrP*20 may contribute to clinical manifestations at the early stage of sporadic CJD in which no significant neuropathological changes are evident and there is no 3F4-detected PrP27–30. However, this suggestion should be received with caution since not all actual pathological changes may be evident in the biopsy samples, which are normally of small size. Nevertheless, detection of the elevated 1E4-detected PrP*20 is important in the early diagnosis of human prion diseases because it may be overlooked if a diagnosis is based only on detection of the 3F4-recognized PrP27–30. Furthermore, whether the accumulation in the brain of the predominant 1E4-detected PK-resistant PrP is associated with a unique form of prion diseases remains to be ascertained. Our preliminary result on a large number of normal cases indicates that no significant correlation exists between aging and the level of PrP*20 [J.Yuan and W. Q. Zou, unpublished data]. However, the effect of aging on the formation of PrP*20 in sporadic CJD remains to be investigated. In addition, it would be intriguing to determine whether this prion-like form plays a role in the pathogenesis of various infectious forms of prion diseases such as variant CJD and iatrogenic CJD and whether PrP*20 is also present in the peripheral tissues of prion-infected subjects. Although it would not be practicable to conduct the study in patients because of the difficulty of early identification of a case with such a rare disease, an animal study to investigate the kinetics of the accumulation of PrP*20 after prion inoculation would be able to address this issue.

Acknowledgements. We are grateful to all the referring physicians and to the Human Brain and Spinal Fluid Resource Center (Los Angeles, CA) for providing non-CJD brain samples. This work was supported in part by the CJD Foundation, STERIS Co., the National Institutes of Health Grants AG-14359 and AG08702, the Centers for Disease Control and Prevention Contract UR8/CCU515004, and the Britton Fund.

1 Prusiner, S. B. (1998) Prions. Proc. Natl. Acad. Sci. U S A 95, 13363–13383.
2 Aguzzi, A. and Polymenidou, M. (2004) Mammalian prion biology: one century of evolving concepts. Cell 116, 313–327.
3 Jarrett, J. T. and Lansbury, P. T. Jr. (1993) Seeding "one-dimensional crystallization" of amyloid: a pathogenic mechanism in Alzheimer's disease and scrapie? Cell 73, 1055–1058.
4 Yuan, J., Xiao, X., McGeehan, J., Dong, Z., Cali, I., Fujioka, H., Kong, Q., Kneale, G., Gambetti, P. and Zou, W. Q. (2006) Insoluble aggregates and protease-resistant conformers of prion protein in uninfected human brains. J. Biol. Chem. 281, 34848–34858.
5 Hall, D. and Edskes, H. (2004) Silent prions lying in wait: a two-hit model of prion/amyloid formation and infection. J. Mol. Biol. 336, 775–786.
6 Parchi, P., Castellani, R., Capellari, S., Ghetti, B., Young, K., Chen, S. G., Farlow, M., Dickson, D. W., Sima, A. A., Trojanowski, J. Q., Petersen, R. B. and Gambetti, P. (1996) Molecular basis of phenotypic variability in sporadic Creutzfeldt-Jakob disease. Ann. Neurol. 39, 767–778.
7 Parchi, P., Zou, W. Q., Wang, W., Brown, P., Capellari, S., Ghetti, B., Kopp, N., Schulz-Schaeffer, W. J., Kretzschmar, H. A., Head, M. W., Ironside, J. W., Gambetti, P. and Chen, S. G. (2000) Genetic influence on the structural variations of the abnormal prion protein. Proc. Natl. Acad. Sci. USA 97, 10168–10172.
8 Kascsak, R. J., Rubenstein, R., Merz, P. A., Tonna-DeMasi, M., Fersko, R., Carp, R. I., Wisniewski, H. M. and Diringer H. (1987) Mouse polyclonal and monoclonal antibody to scrapie-associated fibril proteins. J. Virol. 61, 3688–3693.
9 Peretz, D., Williamson, R. A., Matsunaga, Y., Serban, H., Pinilla, C., Bastidas, R.B., Rozenshteyn, R., James, T. L., Houghten, R. A., Cohen, F. E., Prusiner, S. B. and Burton D. R. (1997) A conformational transition at the N terminus of the prion protein features in formation of the scrapie isoform. J. Mol. Biol. 273, 614–622.
10 Chen, S. G., Teplow, D. B., Parchi, P., Teller, J. K., Gambetti, P. and Autilio-Gambetti, L. (1995) Truncated forms of the human prion protein in normal brain and in prion diseases. J. Biol. Chem. 270, 19173–19180.
11 Nitrini, R., Rosemberg, S., Passos-Bueno, M. R., da Silva, L. S., Iughetti, P., Papadopoulos, M., Carrilho, P. M., Caramelli, P., Albrecht, S., Zatz, M. and LeBlanc, A. (1997) Familial spongiform encephalopathy associated with a novel prion protein gene mutation. Ann. Neurol. 42, 138–146.
12 Farlow, M. R., Yee, R. D., Dlouhy, S. R., Conneally, P. M., Azzarelli, B. and Ghetti, B. (1989) Gerstmann-Sträussler-Scheinker disease. I. Extending the clinical spectrum. Neurology 39, 1446–1452.
13 Ghetti, B., Tagliavini, F., Masters, C. L., Beyreuther, K., Giaccone, G., Verga, L., Farlow, M. R., Conneally, P. M., Dlouhy, S. R., Azzarelli, B. and Bugiani, O. (1989) Gerstmann-Sträussler-Scheinker disease. II. Neurofibrillary tangles and plaques with PrP-amyloid coexist in an affected family. Neurology 39, 1453–1461.
14 Morillas, M., Swietnicki, W., Gambetti, P. and Surewicz, W. K. (1999) Membrane environment alters the conformational

structure of the recombinant human prion protein. J. Biol. Chem. 274, 36859–36865.
15 Fox, D. G., Cary, P. D. and Kneale, G. G. (1999) Conformational studies of the C-terminal domain of bacteriophage Pf1 gene 5 protein. Biochim. Biophys. Acta 1435, 138–146.
16 Bessen, R. A. and Marsh, R. F. (1994) Distinct PrP properties suggest the molecular basis of strain variation in transmissible mink encephalopathy. J. Virol. 68, 7859–7868.
17 Guo, J. P., Petric, M., Campbell, W. and McGeer, P. L. (2004) SARS corona virus peptides recognized by antibodies in the sera of convalescent cases. Virology 324, 251–256.
18 Petersen, R.B., Parchi, P., Richardson, S. L., Urig, C. B. and Gambetti, P. (1996) Effect of the D178N mutation and the codon 129 polymorphism on the metabolism of the prion protein. J. Biol. Chem. 271, 12661–12668.
19 Capellari, S., Zaidi, S. I., Long, A. C., Kwon, E. E. and Petersen, R. B. (2000) The Thr183Ala mutation, not the loss of the first glycosylation site, alters the physical properties of the prion protein. J. Alzheimers Dis. 2, 27–35.
20 Zaidi, S. I., Richardson, S. L., Capellari, S., Song, L., Smith, M. A., Ghetti, B., Sy, M. S., Gambetti, P. and Petersen, R. B. (2005) Characterization of the F198S prion protein mutation: enhanced glycosylation and defective refolding. J. Alzheimers Dis. 7, 159–171.
21 Kretzschmar, H. A., Stowring, L. E., Westaway, D., Stubblebine, W. H., Prusiner, S. B. and Dearmond, S. J. (1986) Molecular cloning of a human prion protein cDNA. DNA 5, 315–324.
22 Zou, W. Q. and Cashman, N. R. (2002) Acidic pH and detergents enhance in vitro conversion of human brain PrPC to a PrPSc-like form. J. Biol. Chem. 277, 43942–43947.
23 Zou, W. Q., Zheng, J., Gray, D. M., Gambetti, P. and Chen, S. G. (2004) Antibody to DNA detects scrapie but not normal prion protein. Proc. Natl. Acad. Sci. U S A 101, 1380–1385.
24 Jiménez-Huete, A., Lievens, P. M., Vidal, R., Piccardo, P., Ghetti, B., Tagliavini, F., Frangione, B. and Prelli, F. (1998) Endogenous proteolytic cleavage of normal and disease-associated isoforms of the human prion protein in neural and non-neural tissues. Am. J. Pathol. 153, 1561–1572.
25 Nitrini, R., Teixeira da Silva, L. S., Rosemberg, S., Caramelli, P., Carrilho, P. E., Iughetti, P., Passos-Bueno, M. R., Zatz, M., Albrecht, S. and LeBlanc, A. (2001) Prion disease resembling frontotemporal dementia and parkinsonism linked to chromosome 17. Arq. Neuropsiquiatr. 59, 161–164.
26 Zou, W. Q., Colucci, M., Gambetti, P. and Chen, S. G. (2003) Characterization of prion proteins. Methods Mol. Biol. 217, 305–314.
27 Yuan, J., Kinter, M., McGeehan, J., Perry, G., Kneale, G., Gambetti, P. and Zou, W. Q. (2005) Concealment of epitope by reduction and alkylation in prion protein. Biochem. Biophys. Res. Commun. 326, 652–659.
28 Zahn, R., Liu, A., Lührs, T., Riek, R., von Schroetter, C., López García, F., Billeter, M., Calzolai, L., Wider, G. and Wüthrich, K. (2000) NMR solution structure of the human prion protein. Proc. Natl. Acad. Sci. U S A 97, 145–150.
29 Cohen, F. E. and Prusiner, S. B. (1998) Pathologic conformations of prion proteins. Annu. Rev. Biochem. 67, 793–819.
30 Prusiner, S. B., Scott, M. R., DeArmond, S. J. and Cohen, F. E. (1998) Prion protein biology. Cell 93, 337–348.
31 Leclerc, E., Peretz, D., Ball, H., Sakurai, H., Legname, G., Serban, A., Prusiner, S. B., Burton, D. R. and Williamson, R. A. (2001) Immobilized prion protein undergoes spontaneous rearrangement to a conformation having features in common with the infectious form. EMBO J. 20, 1547–1554.
32 Tessier, P. M. and Lindquist, S. (2007) Prion recognition elements govern nucleation, strain specificity and species barriers. Nature 447, 556–562.
33 Grasbon-Frodl, E., Lorenz, H., Mann, U., Nitsch, R. M., Windl, O. and Kretzschmar, H. A. (2004) Loss of glycosylation associated with the T183A mutation in human prion disease. Acta Neuropathol. (Berl) 108, 476–484.
34 Piccardo, P., Seiler, C., Dlouhy, S.R., Young, K., Farlow, M. R., Prelli, F., Frangione, B., Bugiani, O., Tagliavini, F. and Ghetti, B. (1996) Proteinase-K-resistant prion protein isoforms in Gerstmann-Sträussler-Scheinker disease (Indiana kindred). J. Neuropathol. Exp. Neurol. 55, 1157–1163.